DOI: 10.1002/ejic.200601130

Synthesis and Characterisation of Polymer-Anchored Oxidovanadium(IV) Complexes and Their Use for the Oxidation of Styrene and Cumene

Mannar R. Maurya,*[a] Umesh Kumar,[a] and P. Manikandan[b]

Keywords: Vanadium(IV) complexes / Polymer support / Heterogeneous catalysts / Oxidations

The Schiff bases H_2fsal-ea (**I**), H_2fsal-pa (**II**) and H_2fsal-amp (**III**), derived from 3-formylsalicylic acid and 2-aminoethanol, 3-aminopropanol and 2-amino-2-methylpropanol, respectively, have been connected, by means of covalent bonds, to chloromethylated polystyrene cross-linked with 5% divinylbenzene. On treatment with [VO(acac)$_2$] in dimethylformamide (DMF), these polymer-anchored ligands PS-H_2fsal-ea (**IV**), PS-H_2fsal-pa (**V**) and PS-H_2fsal-amp (**VI**) gave the oxidovanadium(IV) complexes, PS-[VO(fsal-ea)·DMF] (**4**), PS-[VO(fsal-pa)·DMF] (**5**) and PS-[VO(fsal-amp)·DMF] (**6**), respectively. The corresponding neat complexes [VO(fsal-ea)]$_2$ (**1**), [VO(fsal-pa)]$_2$ (**2**) and [VO(fsal-amp)]$_2$ (**3**) have also been similarly prepared. These complexes all exhibit a medium intensity band between 964 and 993 cm^{-1} in their IR spectra resulting from the V=O stretch. The EPR spectra of the polymer-anchored complexes are characteristics of monomeric V^{IV} centres with a simple $S = ½$ electronic spin and with an axial pattern typical of square pyramidal geometry. Broad features for the neat complexes along with magnetic susceptibility studies suggest the presence of antiferromagnetic exchange interactions between two vanadium centres in close proximity. These catalysts have been tested for the oxidation of styrene and cumene and were found to be efficient. Styrene gives five reaction products namely styrene epoxide, benzaldehyde, 1-phenylethane-1,2-diol, benzoic acid and phenylacetaldehyde, whereas cumene gives acetophenone, 2-phenylpropanal, α-methyl styrene epoxide, 2-phenyl-2-propanol, 2-isopropyl-1,4-benzoquinone and α-methyl styrene. The polymer-anchored heterogeneous catalysts are recyclable. The catalytic activities of the neat complexes have also been examined and compared with the corresponding anchored analogues.

Introduction

Advances in the coordination chemistry of vanadium with multidentate ligands stem from the discovery of the vanadium containing enzymes, namely vanadate-dependent haloperoxidases,[1] vanadium nitrogenases[2] and vanadium containing nitrate reductases.[3] Vanadate-dependent haloperoxidases catalyse the peroxide mediated oxidation of halides to hypohalous acid which further halogenates hydrocarbons in a non-enzymatic process.[4] Many vanadium complexes provide a suitable structural and/or functional model for these enzymes.[5,6] Oxidations of aliphatic as well as aromatic substrates including (prochiral) organic sulfides to (chiral) sulfoxides, catalysed by vanadium complexes, have also been achieved in excellent yield.[7,8]

The catalytic potential of [VO(sal-ohyba)] and [K(H$_2$O)][-VO$_2$(sal-ohyba)] (H_2sal-ohyba = Schiff base derived from salicylaldehyde and *o*-hydroxybenzylamine) for the oxidation and oxidative bromination of organic substrates has been recently investigated in our group.[9] The stability and potential of these complexes to be recycled were improved remarkably by immobilizing them onto a polymer support. For the development of industrial processes, such modifications to homogeneous catalysts would be very important and this, in addition, would lead to operational flexibility of the catalyst as well.[10] Recently, Ando et al. reported oxidovanadium(IV) complexes covalently bonded to Merrifield resin as a heterogeneous catalysts for the oxidation of organic sulfide selectively.[11]

In continuation of our efforts on the development of polymeric supported/anchored vanadium complexes and their catalytic potential, we report herein the preparation and characterisation of polymer-anchored oxidovanadium(IV) complexes of ligands **I**, **II** and **III**, Scheme 1, along with their neat complexes. The catalytic potential of these complexes has been demonstrated by studying the oxidation of styrene and cumene.

[a] Department of Chemistry, Indian Institute of Technology Roorkee,
Roorkee 247667, India
E-mail: rkmanfcy@iitr.ernet.in
[b] Catalysis and Inorganic Chemistry Division, National Chemical Laboratory,
Pune 411008, India
Supporting information for this article is available on the WWW under http://www.eurjic.org or from the author.

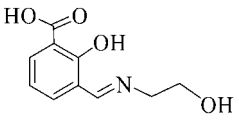

I: H_2fsal-ea

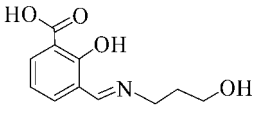

II: H_2fsal-pa

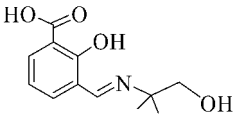

III: H_2fsal-amp

Scheme 1.

Results and Discussion

Synthesis, Reactivity and Solid-State Characteristics

The elemental and spectroscopic data (IR, ^{1}H and ^{13}C NMR) of the ligands H_2fsal-ea (**I**), H_2fsal-pa (**II**) and H_2fsal-amp (**III**) used in the present study, described in the experimental section, confirm the structures of ligands. The chloromethylated polystyrene, cross-linked with 5% divinylbenzene, reacts with these ligands in DMF in the presence of triethylamine to give the polymer-anchored ligands PS-H_2fsal-ea(IV), PS-H_2fsal-pa (**V**) and PS-H_2fsal-amp (**VI**), respectively. During this process the -COOH group of 3-formylsalicylic acid reacts with the -CH_2Cl group of polystyrene. Covalent bonding through the -COOH group of the ligand has been further demonstrated by treating benzylchloride with H_2fsal-ea (**I**) under the above reaction conditions. Scheme 2 depicts the structures of the ligands isolated; a representative synthetic procedure for **IV** is also shown. The remaining chlorine content of 1.7% (0.49 mmol Cl/g of resin) in PS-H_2fsal-ea, 1.8% (0.51 mmol Cl/g of resin) in PS-H_2fsal-pa and 2.2% (0.62 mmol Cl/g of resin) in PS-H_2fsal-amp suggested roughly a 90% load of the ligands.

These anchored ligands react with [VO(acac)$_2$] in DMF at ca. 90 °C to give the polymer-anchored oxidovanadium(IV) complexes PS-[VO(fsal-ea)·DMF] (**4**), PS-[VO(fsal-pa)·DMF] (**5**) and PS-[VO(fsal-amp)·DMF] (**6**) which are dark green in colour. Equation (1) represents the synthetic procedure.

$$\text{PS-H}_2\text{fsal-ea} + [\text{VO(acac)}_2] \xrightarrow{\text{DMF}} \text{PS-[V}^{\text{IV}}\text{O(fsal-ea)·DMF]} + 2\ \text{Hacac} \quad (1)$$

4

Similarly, the reaction of [VO(acac)$_2$] with an equimolar amount of the neat ligands **I**, **II** and **III** in acetonitrile at reflux yields the neat oxidovanadium(IV) complexes [VO(fsal-ea)]$_2$ (**1**), [VO(fsal-pa)]$_2$ (**2**) and [VO(fsal-amp)]$_2$ (**3**), respectively. The neat complexes exhibit effective magnetic moments of 1.31 (for **1**), 1.34 (for **2**) and 1.49 μ_B (for **3**) at 298 K which are lower than the expected value of 1.73 μ_B for a d^1 (S = ½) system. We have also studied the magnetic susceptibilities of these complexes as a function of temperature in the 298–90 K range. Figure 1 shows a plot of the magnetic susceptibility χ_M^{corr} as a function of temperature for **1**. The χ_M^{corr} values show a slight dependence on temperature, the observed magnetic moment values varied in the range 1.31–1.15 μ_B and the Curie–Weiss plot [$1/\chi_M^{corr}$ vs. T], as shown in Figure 2, was found to be a straight line with a Weiss constant of –40. Similarly, the magnetic moment values of **2** and **3** varied in the ranges 1.34–1.10 and 1.49–1.23 μ_B, respectively, with Weiss constant values of ca. –50. These data all indicate an antiferromagnetic interaction possibly due to dimerisation of the complexes.[12,13] Based on the variations in magnetic moments with temperature and the spectroscopic studies of, for example, complexes [VO(X-sal-ea)]$_2$ (where X-sal-ea = Schiff bases derived from salicylaldehyde and 2-aminoethanol or 3-aminopropanol, X = 5-Cl, 5-Br, 5-NO_2, 3-NO_2,

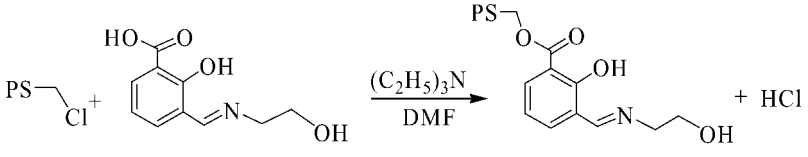

H_2fsal-ea **I**

PS-H_2fsal-ea **IV**

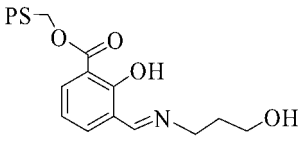

PS-H_2fsal-pa **V**

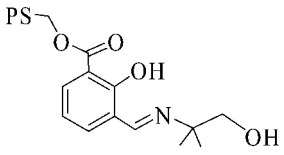

PS-H_2fsal-amp **VI**

Scheme 2. Synthetic procedure for **IV** only; PS represents the backbone of chloromethylated polystyrene.

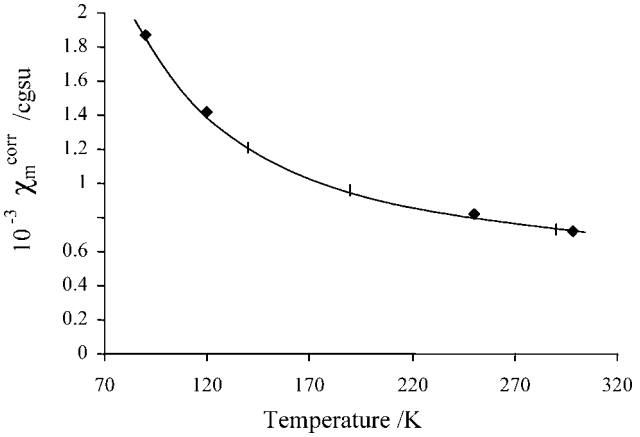

Figure 1. Plot of the magnetic susceptibility χ_m^{corr} vs. temperature for $[VO(fsal\text{-}ea)]_2$ (**1**).

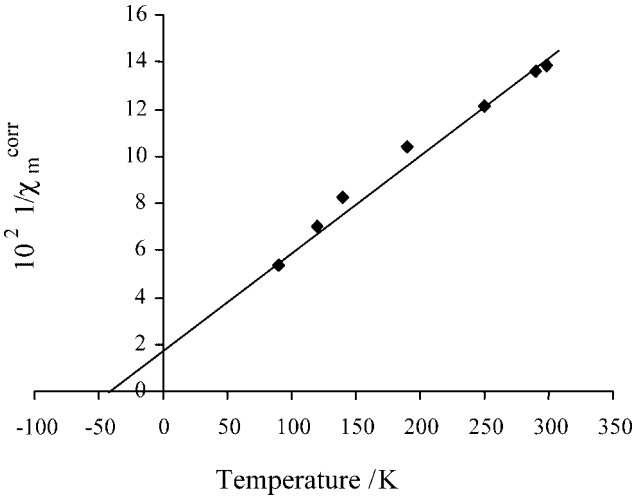

Figure 2. Curie–Weiss plot $[1/\chi_m^{corr}$ vs. $T]$ for $[VO(fsal\text{-}ea)]_2$ (**1**).

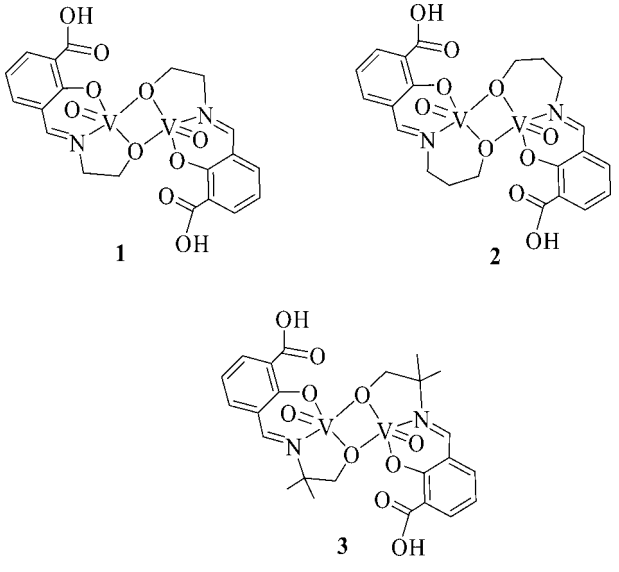

Scheme 3. Proposed structure for neat oxidovanadium(IV) complexes.

5-OMe, 3-OMe), Syamal et al. suggested antiferromagnetic exchange interactions along with a dimeric structure.[14] Thus, the dimeric structure as shown in Scheme 3 for the neat complexes may also be proposed here. A dimeric structure for $[VO(sal\text{-}ea)]_2$ has been confirmed by a single-crystal X-ray diffraction study.[15]

Scanning Electron Micrograph

Scanning electron micrographs (SEM) for a single bead of pure chloromethylated polystyrene, the polymer-anchored ligand and the polymer-anchored vanadium complexes were recorded in order to observe the morphological changes. Images of PS-H_2fsal-ea (**IV**) and PS-[VO(fsal-ea)·DMF] (**4**) are reproduced in Figure 3. As expected, the pure polystyrene bead has a smooth and flat surface while the anchored ligands and complexes show a very slight roughening of the top layer. This roughening is relatively greater in the complexes possibly due to the interaction of vanadium with the anchored ligand which resulted in the formation of complexes with a fixed geometry. Accurate information on the morphological changes in terms of the exact orientation of the ligands coordinated to the metal ion has not been possible due to poor loading of the metal complex.

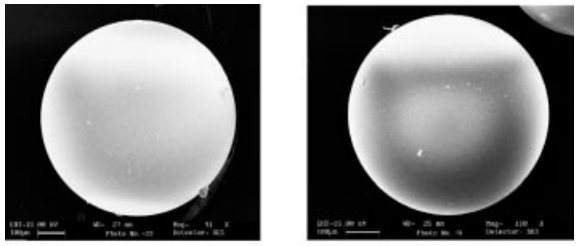

Figure 3. Scanning Electron Micrographs (SEM) of PS-H_2fsal-ea (**IV**) and PS-[VO(fsal-ea)·DMF] (**4**); magnification ca. ×200.

TGA Study

Thermogravimetric analyses in an oxygen atmosphere showed good stabilities for polymer-anchored complexes **4**, **5** and **6** up to ca. 175 °C. The first weight loss starting just above 175 °C is possibly due to the loss of coordinated DMF. The complexes, thereafter, decompose in multiple steps. Quantitative measurement of weight loss at various stages was not possible due to the overlapping nature of the decompositions. However, the stabilities of the final residues at ca. 700 °C suggest the formation of V_2O_5. The metal content calculated from the final residue in each case was close to that recorded by atomic absorption spectroscopy.

IR Spectroscopic Study

The experimental section contains a partial list of the IR spectroscopic data of all ligands and complexes. The chloromethylated polystyrene exhibits strong peaks at 1264 and

673 cm^{-1} due to CH_2Cl group and the absence of these peaks in the polymer-anchored ligands suggests covalent bonding of the chloromethylated polystyrene to the ligands.[16] A sharp band due to ν(C=O) of the carboxylate group appears at 1670–1676 cm^{-1} in the polymer-anchored ligands and complexes. In the corresponding neat ligands and complexes, this band appears at either the same or a slightly lower wavenumber. The ν(C=N) (azomethine) stretch of the neat ligands mostly appears along with the ν(C=O). However, a sharp peak due to the ν(C=N) (azomethine) stretch is observable in the spectra of the corresponding complexes at a lower wavenumber. The polymer-anchored ligands show a medium intensity band at 1630–1635 cm^{-1} and this band shifts to a lower wavenumber by ca. 30 cm^{-1} in the complexes thereby indicating the coordination of the azomethine nitrogen atom. The coordination of phenolic oxygen could not be assigned unequivocally in most complexes because of the appearance of a weak broad band in the 3400 cm^{-1} region. Similarly, coordination of DMF in **4**, **5** and **6** could not be possible because of the strong ν(C=O) absorption band of the carboxylate in the same region. In addition to this, all the complexes exhibit a sharp ν(V=O) band in the 964–993 cm^{-1} region.[6]

Electronic and Fluorescence Spectroscopic Studies

The electronic spectra of the neat and anchored complexes in Figure S1 and relevant data in Table S2 are given in the Supporting Information (see also the footnote on the first page of this article). The spectroscopic patterns shown by the neat as well as the supported ligands are essentially the same except for the broadness of the bands in nujol. The expected charge-transfer band at ca. 400 nm could not be distinguished due to the appearance of an n→π* transition in the same region. In addition, two additional weak bands at ca. 570 and 690 nm were observed for neat complexes in DMF due to d-d transitions thus indicating the presence of a vanadium(IV) ion at the centre.

The fluorescence excitation and emission spectra of 10^{-6} M methanolic solution of oxidovanadium(IV) complexes **1**, **2** and **3** were recorded at room temperature and are presented in Figure 4. All neat complexes have approximately the same chromophore units and exhibit similar spectroscopic patterns. On excitation at 257 nm (in the UV region) complex **1** exhibited a strong band at λ_{max} = 483 nm (in the visible region) with a shoulder band at 556 nm and, on excitation at 387.5 nm, exhibited a broad peak with λ_{max} = 501 nm. In the case of complexes **2** and **3**, excitation at 258 (in **2**) and 255 (in **3**) nm gave emission bands at 464 and 466 nm, respectively, along with weak shoulder bands at 517 and 554 nm. Similarly, broad peaks at 503 (in **2**) and 502 nm (in **3**) were obtained with excitation at 382 and 385.5 nm, respectively. As, expected, the overtone at ca. 510 nm was observed as a sharp band in all complexes. All these spectroscopic patterns hint towards the photo-catalytic utility of these complexes.

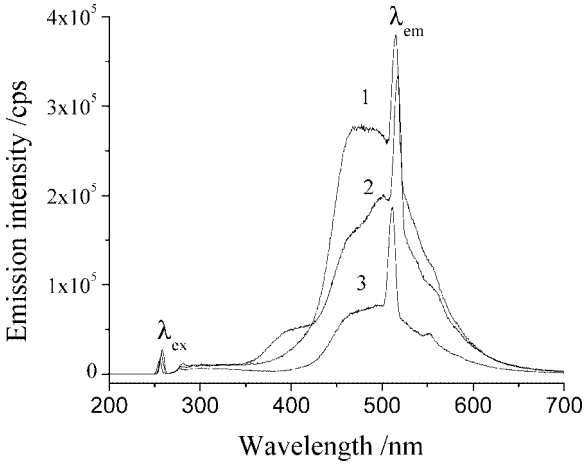

Figure 4. Emission spectra of complexes $[VO(fsal\text{-}ea)]_2$ (**1**), $[VO(fsal\text{-}pa)]_2$ (**2**) and $[VO(fsal\text{-}amp)]_2$ (**3**) recorded in methanol at ambient temperature.

EPR Spectroscopic Study

The room temperature X-band EPR spectra of the polymer-anchored samples are reproduced in Figure 5. They are characteristics of monomeric V^{IV} centres with a simple S = ½ electronic spin and a typical axial pattern for a possible square pyramidal geometry, Scheme 4. The hyperfine features are well resolved in both the parallel and perpendicular regions. These resolved hyperfine features reflect the fact that the vanadium centres are well separated by the polymer backbones which causes least dipolar vanadium–vanadium coupling. Such arrangements generally broaden the EPR pattern. The hyperfine lines are typical for an interaction of the unpaired electron of the vanadium(IV) ion with its nucleus, ^{51}V having a high abundance of 99.75% and a nuclear

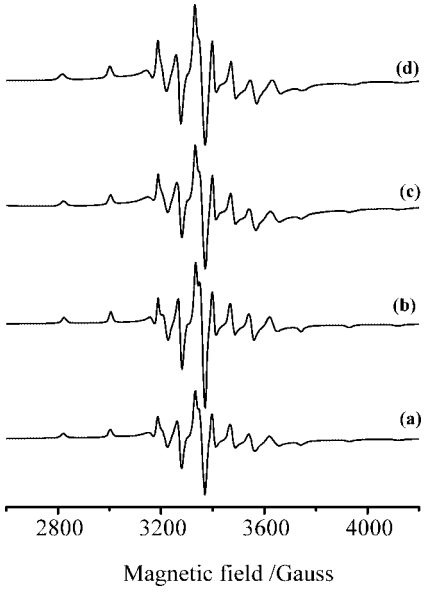

Figure 5. Room temperature EPR spectra of polymer-anchored complexes (a) PS-[VO(fsal-ea)·DMF] (**4**), (b) PS-[VO(fsal-pa)·DMF] (**5**), (c) PS-[VO(fsal-amp)·DMF] (**6**) and (d) PS-[VO(fsal-pa)·DMF] (**5**) (recovered); the microwave frequency was 9.4458 GHz.

spin $I = {}^{7}/_{2}$. The anisotropic EPR spectrum of the V^{IV} ion with $g_{\|} < g_{\perp}$ and $A_{\|} > A_{\perp}$ is characteristic of square pyramidal complexes with possible C_{4v} symmetry in which the V=O bond is along the z axis and the other four coordinating atoms are along the x and y axes.[17] Simulation of the EPR spectra was carried to extract the Hamiltonian parameters and the resultant parameters are given in Table 1. As seen in the table and Figure 5, the Hamiltonian parameters are more or less the same for the all three polymer-anchored samples indicating that local symmetry and environments around the V centres are more or less the same.

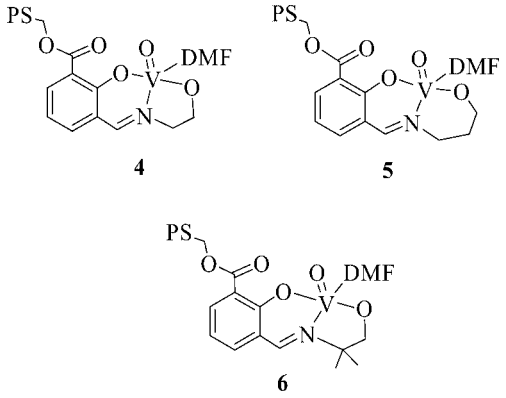

Scheme 4. Possible structure for polymer-anchored complexes.

After carrying out the catalytic reactions, the polymer-anchored catalysts were filtered, washed with acetonitrile and dried. The EPR spectra were then recorded under identical conditions. The EPR spectrum for one of the recovered catalysts, PS-[VO(fsal-amp)·DMF] (**6**), is also reproduced in Figure 5 as a representative example. The EPR spectra of the recovered (spent) samples were only slightly different from the fresh samples indicating the environment and coordination geometry of the vanadium centres is retained to the maximum extent after the catalytic reaction. A slight increase in the $A_{\|}$ component for the recovered catalyst can be observed from 18.6 mT to 18.8 mT. A higher $A_{\|}$ value is generally due to reduced delocalisation of the paramagnetic electron density of the V centre indicating a slight displacement in the coordinating atom of the ligand. In other words, the vanadium–nitrogen bond is slightly weaker than that in the neat compound.

The EPR spectra for the neat compounds were also recorded and are reproduced in Figure 6. The broad spectroscopic features are typical for dimeric or polymeric species with dipolar interactions or exchange interactions with V^{4+}–V^{4+} pairs with spin $S = 1$.[18] In the absence of any hyperfine features, the spectra could be best fitted by superimposing features of at least two V^{4+}–V^{4+} pairs having slightly different environments with different zero-field splitting parameters, D and E, and the resultant parameters are given in Table 1. As seen in the table, one of the V^{4+}–V^{4+} pairs has a D value in the range 1850–1900 MHz and an E value of 500 MHz indicating a strong rhombic distortion site. The other species could be fitted with D in the range 1250–1350 MHz with no E splitting thus indicating less distortion. The broad features in the EPR spectra for the complexes $[VO(X\text{-sal-ea})]_2$ (X = 5-Cl, 5-Br, 5-NO_2, 5-OMe, 3-OMe) have also been noted previously and interpreted on the basis of the presence of antiferromagnetic exchange interactions between two vanadium centres in close proximity.[12–14]

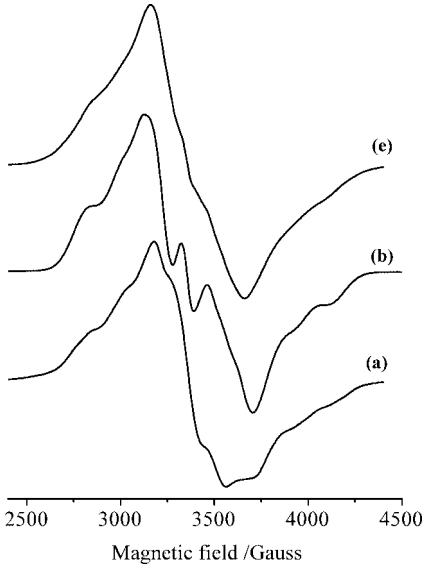

Figure 6. Room temperature EPR spectra of neat complexes (a) $[VO(fsal\text{-}ea)]_2$ (**1**), (b) $[VO(fsal\text{-}pa)]_2$ (**2**) and (c) $[VO(fsal\text{-}amp)]_2$ (**3**).

Table 1. Spin Hamiltonian parameters for the calculated EPR spectra: g-tensors ($g_{\|}$, $g_{\perp}$), hyperfine tensors ($A_{\|}$, $A_{\perp}$), zero-field splitting parameters (D, E).

Compound	Spectrum	$g_{\|}$ (g_{iso})	$g_{\perp}$	$A_{\|}$ (A_{iso}) (mT)	$A_{\perp}$ (mT)	D (MHz)	E (MHz)
PS-[VO(fsal-ea)·DMF] (**4**)	1	1.945	1.999	18.6	7	–	–
PS-[VO(fsal-pa))·DMF] (**5**)	1	1.945	1.999	18.4	7	–	–
PS-[VO(fsal-amp))·DMF] (**6**)	1	1.945	1.999	18.6	7	–	–
PS-[VO(fsal-pa))·DMF] (**5**) (recovered)	1	1.943	1.999	18.8	7	–	–
$[VO(fsal\text{-}ea)]_2$ (**1**)	1	1.955	–	–	–	1250	0
	2	1.940	–	–	–	1190	500
$[VO(fsal\text{-}pa)]_2$ (**2**)	1	1.975	–	–	–	1150	0
	2	1.940	–	–	–	1850	500
$[VO(fsal\text{-}amp)]_2$ (**3**)	1	1.975	–	–	–	1350	0
	2	1.940	–	–	–	1850	500

Catalytic Activity Study

The catalytic potential of the polymer-anchored as well as the neat complexes were studied for the oxidation of styrene and cumene.

Oxidation of Styrene

Oxidation of styrene catalysed by the polymer-anchored complexes PS-[VO(fsal-ea)·DMF] (**4**), PS-[VO(fsal-pa)·DMF] (**5**) and PS-[VO(fsal-amp)·DMF] (**6**) gave styrene oxide, benzaldehyde, benzoic acid, phenylacetic acid and 1-phenylethane-1,2-diol as indicated in Scheme 5. These reaction products are common and have also been identified earlier by other workers.[19–21]

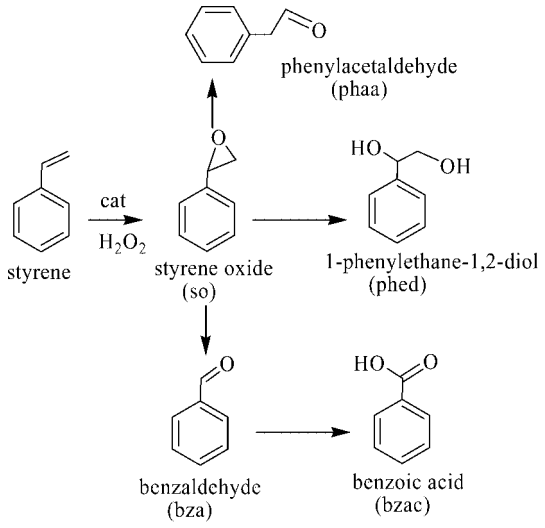

Scheme 5.

Complex **5** was taken as a representative amongst these catalysts and its catalytic activity was studied as a function of the amount of H_2O_2 (mol of H_2O_2 per mol of styrene) and catalyst as well as the temperature of the reaction mixture. These parameters were varied in order to obtain suitable reaction conditions for the maximum oxidation of styrene. Reactions were carried out with three different molar ratios of 1:1, 1:1.5 and 1:2 of styrene to aqueous 30% H_2O_2 for a fixed amount of styrene (1.04 g, 10 mmol) and catalyst (0.040 g) in CH_3CN (10 mL) at 80 °C. The results were analysed periodically for up to 6 h. As illustrated in Figure 7, a maximum conversion of 42% was achieved in 6 h with a styrene to H_2O_2 molar ratio of 1:1. On increasing the ratio to 1:1.5 the conversion was improved to 65% while a 1:2 molar ratio showed a maximum conversion of 95%. No further improvement in the oxidation was observed on increasing the molar ratio to 1:3 (not shown in Figure) which suggests that a large amount of oxidant is not an essential condition for improving the oxidation of styrene. In another experiment, three different catalyst loadings, viz. 0.030, 0.040 and 0.070 g, were varied at styrene to H_2O_2 ratios of 1:2 under the above reaction conditions and the results are shown in Figure 8. As seen in the figure, 0.030 g of catalyst gave only a 52.5% conversion while catalyst loadings of 0.040 and 0.070 g showed maximum conversions of 95 and 97.3%, respectively, at the end of the 6 h. Thus, at the expense of H_2O_2, 0.040 g of catalyst was found to be sufficient to carry out the reaction. The temperature of the reaction mixture also influenced the performance of the catalyst. Figure 9 shows the effect of the reaction temperature on the performance of the catalysts and at 80 °C a much better conversion was achieved.

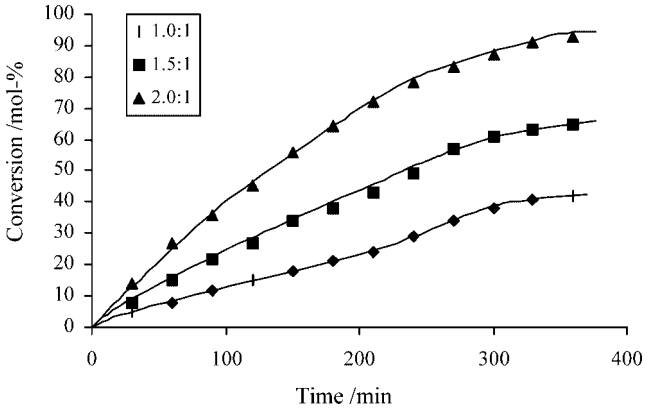

Figure 7. Effect of amount of H_2O_2 on the oxidation of styrene. Reaction conditions: styrene (1.04 g, 10 mmol), PS-[VO(fsal-pa)·DMF] (**5**) (0.040 g), CH_3CN (10 mL) and temp. (80 °C).

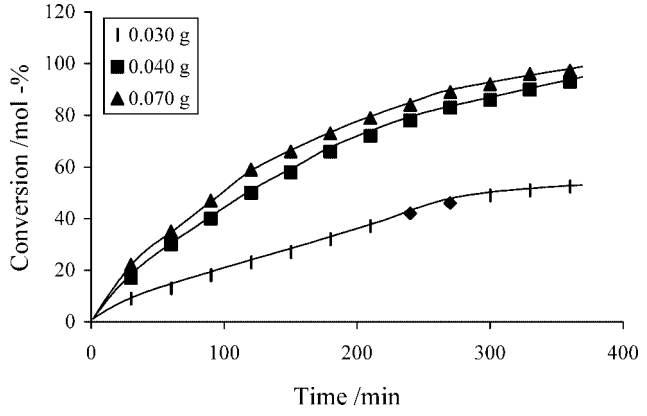

Figure 8. Effect of amount of catalyst on the oxidation of styrene. Reaction conditions: styrene (1.04 g, 10 mmol), H_2O_2 (2.27 g, 20 mmol), CH_3CN (10 mL) and temp. (80 °C).

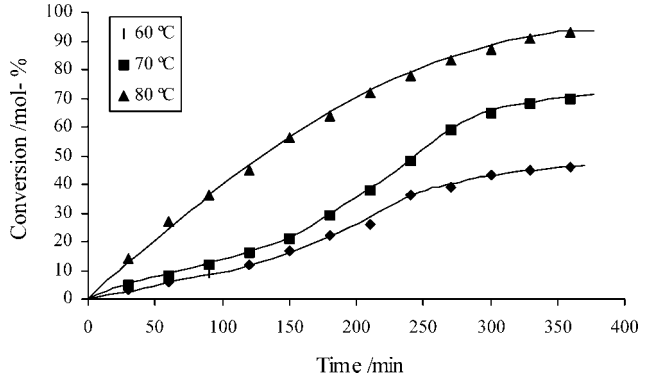

Figure 9. Effect of temperature on the oxidation of styrene. Reaction conditions: styrene (1.04 g, 10 mmol), PS-[VO(fsal-pa)·DMF] (**5**) (0.040 g), H_2O_2 (2.27 g, 20 mmol) and CH_3CN (10 mL).

Other catalysts e.g. **4** and **6** were tested under the reaction conditions as optimised above. Thus, for 10 mmol of substrate, aqueous 30% H_2O_2 (20 mmol) and catalyst (0.040 g) were added in CH_3CN (10 mL) and the reaction was carried out at 80 °C. Table 2 shows a comparison of percent conversion of styrene and the selectivity of various reaction products along with the turnover frequency of the catalysts. Catalyst **4** exhibits a 90% conversion of styrene while **6** exhibits only an 82% conversion. Thus, the performances of these catalysts follow the order: **5** (95%) > **4** (90%) > **6** (82%). The good performance of these catalysts is possibly due to easy formation of peroxo species in the presence of H_2O_2 (vide infra) as well as the ease in transferring oxygen from the intermediate peroxo species to the substrate.

We also tested the catalytic activity of the neat complexes for the oxidation of styrene. Their performances after 6 h are also presented in Table 2. Figure 10 provides conversion percentages for each catalyst as a function of time. For 0.020 g of each the neat vanadium complexes **1**, **2** and **3**, and with reaction conditions fixed as above, the obtained conversions were 65, 70 and 62%, respectively. Their calculated turnover frequencies vary in the range 15.3–17.6 h^{-1}. Thus, the catalytic performances of the neat complexes are also good. However, in the light of special features e.g. easy recovery, no leaching and the ability of the polymer-anchored complexes to be recycled, it may be concluded that polymer-anchored vanadium complexes are better catalysts.

The product selectivity for the polymer-anchored complexes follows the order: benzaldehyde > 1-phenylethane-1,2-diol > benzoic acid > styrene oxide > phenylacetaldehyde while for the neat complexes the order is: benzaldehyde > benzoic acid >1-phenylethane-1,2-diol > styrene oxide > phenylacetaldehyde. The formation of benzaldehyde in the highest yield is possibly due to a nucleophilic attack of H_2O_2 on styrene oxide formed in the first step followed by a cleavage of the intermediate hydroperoxystyrene as shown in Scheme 6. Benzaldehyde formation may also be facilitated by direct oxidative cleavage of the styrene side chain double bond by a radical mechanism.[19] Formation of other products such as benzoic acid from benzaldehyde is rather slow in all reactions. Similarly the formation of phenylacetaldehyde, a product formed by isomerisation of styrene oxide, is less in all cases. Water present in H_2O_2 is probably responsible for the hydrolysis of styrene oxide to 1-phenylethane-1,2-diol to some extent. Low formation of styrene oxide, an important product, is understandable because of its further conversion into other products.

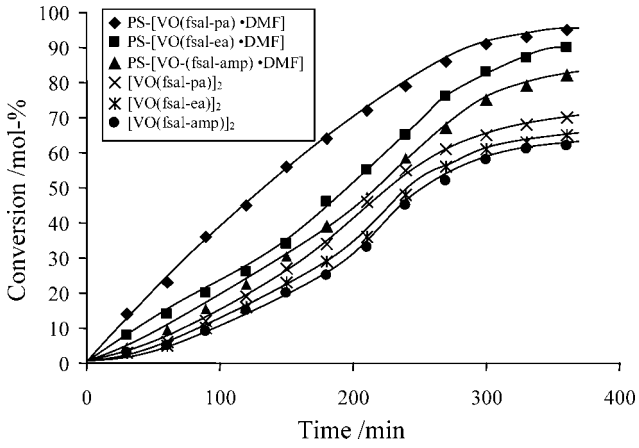

Figure 10. Catalytic comparison of polymer-anchored and neat complexes for the oxidation of styrene. Reaction conditions: styrene (1.04 g, 10 mmol), catalyst (0.040 g for polymer anchored and 0.020 g for neat complexes), H_2O_2 (1.27 g, 20 mmol), CH_3CN (10 mL) and temp. (80 °C).

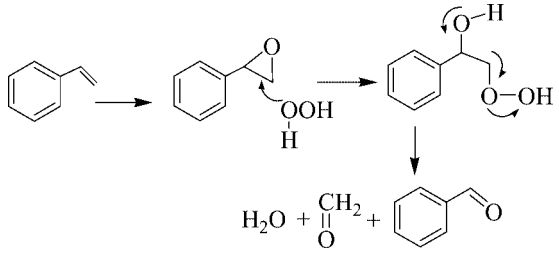

Scheme 6.

Several other polymer-anchored oxidovanadium(IV) complexes e.g. PS-[VO(hmbmz)$_2$] [where PS-Hhmbmz = polymer-anchored 2-(α-hydroxymethyl)benzimidazole],[22] PS-K[VO(O$_2$)$_2$(2-pybzm)] [where 2-pybzm = 2-(2-pyridyl)-benzimidazole][20] and PS-[VO(sal-ohyba)·DMF][9] have been used as catalysts in our laboratory for the oxidation of styrene. Though all these catalysts gave all five products with nearly similar selectivity patterns, the conversions with the catalysts reported here are higher.

Table 2. Turn over frequencies of various catalysts, percent conversion of styrene and product selectivities.

Catalyst	Conv. /mol-%	TOF /h^{-1}	Selectivity /mol-%					
			so[a]	phaa[b]	bza[c]	bzac[d]	phed[e]	Others
[VO(fsal-ea)]$_2$ (**1**)	65	15.3	3.9	3.1	61.7	18.3	8.8	4.3
[VO(fsal-pa)]$_2$ (**2**)	70	16.4	3.6	3.8	62.5	17.2	8.8	4.2
[VO(fsal-amp)]$_2$ (**3**)	62	17.6	3.9	3.4	60.4	18.8	8.9	4.6
PS-[VO(fsal-ea)·DMF (**4**)	90	22.5	4.1	2.9	58.4	7.6	23.5	3.5
PS-[VO(fsal-pa)·DMF] (**5**)	95	25.5	3.8	3.5	62.8	8.7	17.3	3.8
PS-[VO(fsal-amp)·DMF] (**6**)	82	24.0	4.3	3.9	60.6	9.0	18.3	4.0

[a] Styrene epoxide. [b] Phenylacetaldehyde. [c] Benzaldehyde. [d] Benzoic acid. [e] 1-Phenylethane-1,2-diol. Reaction conditions as mentioned in Figure 10.

Oxidation of Cumene

Oxidation of cumene by the polymer-anchored complexes **4**, **5** and **6** gave acetophenone, 2-phenylpropanal, α-methylstyrene epoxide, 2-phenyl-2-propanol, 2-isopropyl-1,4-benzoquinone and α-methylstyrene, as indicated in Scheme 7.

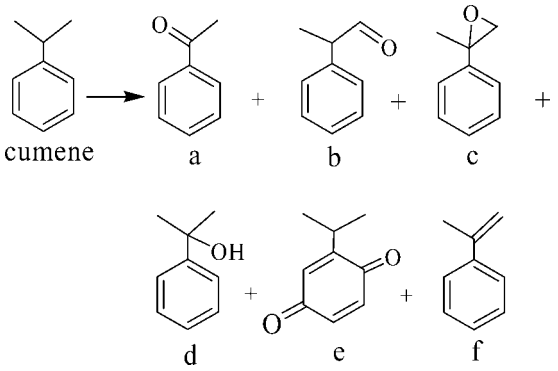

Scheme 7. a = acetophenone, b = 2-phenylpropanal, c = α-methylstyrene epoxide, d = 2-phenyl-2-propanol, e = 2-isopropyl-1,4-benzoquinone and f = α-methylstyrene.

In order to achieve suitable reaction conditions for the maximum oxidation of cumene, complex **5** was taken as a representative catalyst and three different parameters were varied, viz. the amounts of H_2O_2 (mol of H_2O_2 per mol of cumene) and catalyst as well as the temperature of the reaction mixture. The effect of H_2O_2 concentration on the oxidation of cumene is illustrated in Figure 11. A conversion of about 13% was achieved at a cumene to 30% H_2O_2 molar ratio of 1:1 in 6 h when cumene (1.20 g, 10 mmol), 30% H_2O_2 (1.14 g, 10 mmol) and catalyst (0.060 g) were placed in acetonitrile (10 mL) and the reaction was carried out at 80 °C. This conversion improved to ca. 18% on increasing the ratio to 1:1.5 and to 41% at a cumene to 30% H_2O_2 molar ratio of 1:2. This oxidation remained nearly constant on further increasing the amount of oxidant which suggests that a 1:2 (cumene to oxidant) ratio is sufficient enough to maximise the oxidation of cumene.

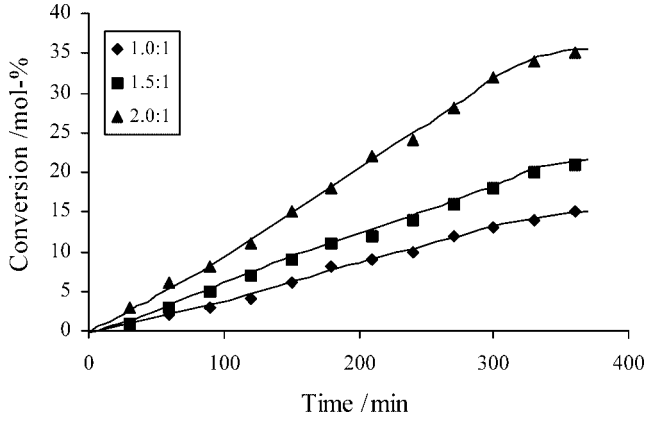

Figure 11. Effect of amount of H_2O_2 on the oxidation of cumene. Reaction conditions: cumene (1.20 g, 10 mmol), PS-[VO(fsal-pa)·DMF] (**5**) (0.060 g), CH_3CN (10 mL) and temp. (80 °C).

Similarly, for a cumene to H_2O_2 ratio of 1:2, three different amounts of catalyst were used, viz. 0.040, 0.060 and 0.080 g, under above reaction conditions and the results are summarised in Figure 12. An amount of 0.040 g of catalyst gave only a 29% conversion while 0.060 g and 0.080 g of catalyst showed maximum conversions of 41 and 44%, respectively. Since the conversion is not significantly higher using 0.080 g of catalyst, an amount of 0.060 g of catalyst can be considered sufficient to carry out the oxidation. Moreover, the turnover rates of the catalyst for the catalytic conversions using 0.060 g and 0.080 g are comparable (7.32 h^{-1} for 0.060 g and 5.9 h^{-1} for 0.080 g). As observed in the case of styrene oxidation, a temperature of at least 80 °C was required to carry out the above reaction effectively. Moreover, time required in achieving the maximum conversion was also reduced on carrying out the reaction at 80 °C.

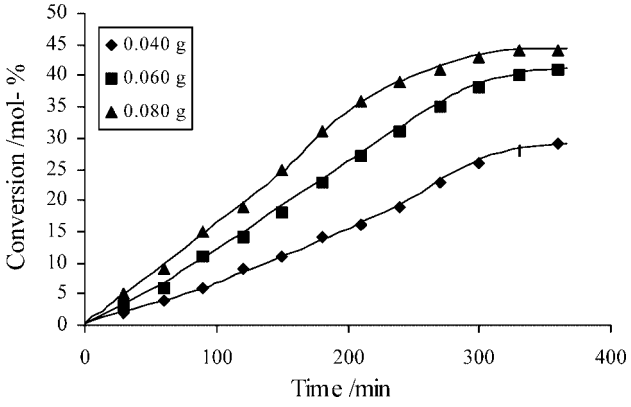

Figure 12. Effect of amount of catalyst PS-[VO(fsal-pa)·DMF] on the oxidation of cumene. Reaction conditions: cumene (1.20 g, 10 mmol), H_2O_2 (2.27 g, 20 mmol), CH_3CN (10 mL) and temp. (80 °C).

Thus, suitable reaction conditions for the maximum oxidation of cumene were fixed as follows: cumene (1.20 g, 10 mmol), 30% H_2O_2 (2.27 g, 20 mmol), catalyst (0.060 g), acetonitrile (10 mL) and a temperature of 80 °C. Catalysts **4** and **6** were also tested under the above optimised reaction conditions and results are summarised in Table 3. Figure 13 shows a comparison of the percentage conversions of all three catalysts as a function of time. The conversion percentages of cumene after 6 h follow the order: **5** (41%) > **4** (39%) > **6** (35%). Independent of the type of catalyst, the percent yield of various products follow the order: acetophenone > 2-phenyl-2-propanal > α-methylstyrene epoxide > 2-phenylpropanol > 2-isopropyl-1,4-benzoquinone ≈ α-methylstyrene.

We have also compared the catalytic activity of these polymer-anchored complexes with their respective neat ones. Table 3 shows a comparison of the percentage conversion of cumene as well as product selectivity of various catalysts obtained after a reaction time of 6 h. For 0.030 g of each of the neat vanadium complexes and keeping other reaction conditions fixed as above, oxidation of cumene in

Table 3. Percent conversion of cumene and selectivity of various oxidation products.

Catalyst	Conv. /mol-%	TOF /h^{-1}	Selectivity /mol-%						
			a[a]	b	c	d	e	f	Others
$[VO(fsal\text{-}ea)]_2$ (**1**)	25	3.92	62	18	10	4	3	2	1
$[VO(fsal\text{-}pa)]_2$ (**2**)	27	4.46	63	19	9	3	2	2	2
$[VO(fsal\text{-}amp)]_2$ (**3**)	21	3.52	66	17	8	3	2	3	1
PS-[VO(fsal-ea)·DMF (**4**)	39	6.50	60	13	17	3	2	3	3
PS-[VO(fsal-pa)·DMF] (**5**)	41	7.32	63	13	14	4	2	2	1
PS-[VO(fsal-amp)·DMF] (**6**)	35	6.83	59	12	17	3	3	2	3

[a] a = acetophenone, b = 2-phenylpropanal, c = α-methylstyrene epoxide, d = 2-phenyl-2-propanol, e = 2-isopropyl-1,4-benzoquinone, f = α-methylstyrene.

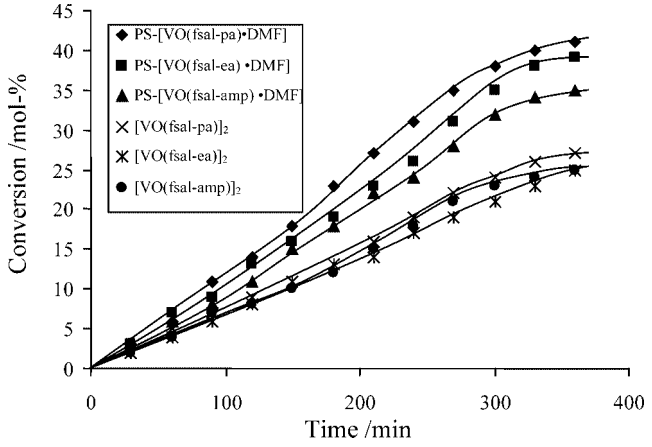

Figure 13. Catalytic comparison of catalysts for the oxidation of cumene. Reaction conditions: cumene (1.20 g, 10 mmol), catalyst (0.060 g), H_2O_2 (2.27 g, 20 mmol), CH_3CN (10 mL), temp. (80 °C).

the 21–27% range was observed which is less than the corresponding values recorded for the anchored complexes. The percentage yields of various products follow the order: acetophenone > 2-phenylpropanal > α-methylstyrene epoxide > 2-phenyl-2-propanol ≈ 2-isopropyl-1,4-benzoquinone ≈ α-methylstyrene. Thus, the yield of α-methylstyrene epoxide is slightly better than 2-phenyl-2-propanal in the case of the neat complexes. However, the selectivity as well as the yield of the major product acetophenone is comparable in all cases.

Homogeneous catalysts such as metal complexes[23] and metalloporphyrins,[24] and heterogeneous catalysts such as platinum metals,[25] metal oxides,[26] metal oxides supported on alumina[27] and metals or metal oxides supported MCM-41[28] have been used for the oxidation of cumene. Only limited literature deals with the oxidation of cumene using polymer-supported catalysts e.g. metal salts[29] and $[Fe(phen)_2]^{2+}$ (phen = phenanthroline)[30] supported on a polymer. Catalytic activity of the complexes reported here compares well with the literature data. However, cumene hydroperoxide, in most cases, has been reported to be the major product amongst the various products formed whereas we observed the formation of acetophenone with a selectivity of 59–66%. This difference is possibly due to the use of different oxidants as well as different metal centres in catalysts.

Proposed Mechanism

As observed earlier, the reaction of cumene proceeds by means of a radical mechanism if molecular oxygen is used as the oxidant. The cumene radical, formed by abstracting the tertiary hydrogen of the cumene by a metal ion, reacts with molecular oxygen to produce an alkyl peroxide, which in turn abstracts hydrogen from cumene to form hydroperoxide (Scheme 8).[28,31] The oxidant H_2O_2 is likely to form peroxidovanadium(V) species with the oxidovanadium(IV) complexes reported here, which finally transfer oxygen to the substrate to give the various products. As cumene hydroperoxide was not observed among the reaction products, the reaction pathway either does not follow any secondary mechanism, e.g. through radical formation, or the cumene hydroperoxide, if formed at all, decomposes catalytically to yield acetophenone and other products.

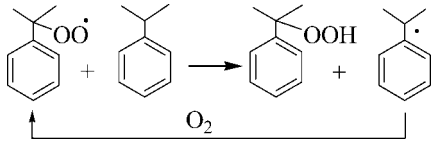

Scheme 8.

Similarly, the formation of styrene oxide may proceed through the transfer of oxygen from oxidoperoxidovanadium(V) species to styrene. The oxidoperoxido species is finally converted to dioxidovanadium(V) and the catalytic cycle moves through these intermediates. These are the most common species observed during the catalytic action of oxidovanadium(IV)/dioxidovanadium(V) complexes for most oxidation reactions carried out in the presence of peroxide.[5a,7b] As the recovered species is EPR active, it seems that dioxidovanadium(V) species are slowly converted to oxidovanadium(IV) during the washing and drying processes and exhibit EPR spectroscopic patterns similar to that of the neat oxidovanadium(IV) complex (cf. Figure 5).

To support the reaction mechanism through peroxidovanadium(V) species formation, we tried the isolation of neat peroxidovanadium(V) complexes with ligands **I**, **II** and **III** but were unsuccessful possibly due to their poor stability at ambient temperature. Nevertheless, the generation of the oxido-monoperoxidovanadium(V) complex, $[VO(O_2)(fsal\text{-}pa)]^-$ has been established in methanol by electronic absorption spectroscopy. In a typical reaction, 10 mL of a ca.

1×10^{-4} M solution of $[VO(fsal\text{-}pa)]_2$ (**2**) was treated with one drop portions of 30% H_2O_2 dissolved in methanol and the resultant spectroscopic changes are presented in Figure 14 Thus, the intensity of the 390 nm band increases slowly along with a corresponding shift to 399 nm by dropwise addition of H_2O_2 dissolved in methanol. The shoulder band at 279 nm does not change its position but undergoes an increase in intensity. Two other bands centred at 255 and 212.5 nm remain constant while a shoulder band at 223 nm slowly appears. We have interpreted this result in terms of the formation of the oxidoperoxidovanadium(V) complex $[VO(O_2)(sal\text{-}pa)]^-$.

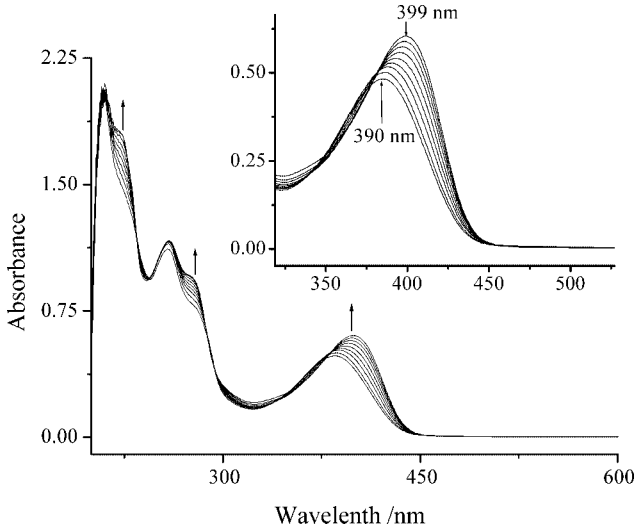

Figure 14. Titration of $[VO(fsal\text{-}pa]_2$ (**2**) with 30% H_2O_2; the spectra were recorded after the successive addition of 1-drop portions of H_2O_2 dissolved in methanol to 10 mL of ca. 10^{-4} M solution of **2** in methanol.

Similar spectroscopic patterns were also observed for complexes **1** and **3**. Oxidoperoxidovanadium(V) complexes have also been generated previously on treatment of, for example, complexes [VO(sal-ohyba)][9] and $K[VO_2(sal\text{-}inh)(H_2O)]$[32] with H_2O_2 in methanol.

Leaching and Heterogeneity of the Catalytic Reaction and Potential of the Catalyst to be Recycled

The polymer-anchored complexes **4**, **5** and **6** have been tested for their ability to be recycled. The reaction mixture was filtered after a contact time of 6 h. The catalysts separated from the reaction mixture after catalytic action in all three cases were washed with acetonitrile, dried and subjected to further catalytic reactions under similar conditions. No appreciable loss in the activity in all cases suggests that catalysts were active even after the first cycle. During catalytic oxidation of styrene and cumene, the solid catalyst was separated from the reaction mixture by filtration after 2 h and the reaction was continued for a further 4 h. The gas chromatographic analyses showed barely a 1% increment in the conversion. This confirms no leaching of the catalyst during the catalytic reaction. No further oxidation of substrates on removal of the solid catalysts is consistent with a heterogeneous process.

Conclusions

Polymer-anchored oxidovanadium(IV) complexes with polymer-anchored ligand PS-H_2fsal-ea, PS-H_2fsal-pa and PS-H_2fsal-amp, having potential catalytic activities for the oxidation of styrene and cumene, have been isolated and characterised. The oxidation of styrene follows the order: PS-[VO(fsal-pa)·DMF] (95%) > PS-[VO(fsal-ea)·DMF] (90%) > PS-[VO(fsal-amp)·DMF] (82%) where the selectivity of the five different products follows the order: benzaldehyde > 1-phenylethane-1,2-diol > benzoic acid > phenylacetaldehyde > styrene oxide. The oxidation of cumene gives at least six different products with the following order of selectivity: acetophenone > 2-phenyl-2-propanal > α-methylstyrene epoxide > 2-phenylpropanol > 2-isopropyl-1,4-benzoquinone and α-methylstyrene. The good performance of these catalysts is possibly due to the facile formation of peroxido species in the presence of H_2O_2 as well as the ease in transferring oxygen from the intermediate peroxido species to the substrate. However, complexes slowly convert back to the oxidovanadium(IV) species since the recycled species exhibit similar EPR spectroscopic patterns. The catalytic activities of these complexes have also been compared with the corresponding neat complexes and it was observed that the neat complexes are, however, good catalyst but exhibit less catalytic activity than the anchored ones. The easy separation of the polymer anchored complexes from the reaction mixture and their ability to be recycled makes them better catalyst compared wit the neat ones. They can pass through up to three cycles without significant loss in their catalytic activities.

Experimental Section

Materials: Analytical reagent grade V_2O_5, (Loba Chemie, India), salicylaldehyde, acetylacetone (Ranbaxy, India), styrene, cumene, 3-aminopropanol (Acros organics, USA), 2-aminoethanol, 2-amino-2-methylpropanol (S.D. Fine Chemicals, India), aqueous 30% H_2O_2 (Qualigens, India) were used as obtained. Other chemicals and solvents were of AR grade. Chloromethylated polystyrene [18.9% Cl (5.3 mmol Cl per gram of resin)] cross-linked with 5% divinylbenzene was obtained as gift from Thermax limited, Pune, India. $[VO(acac)_2]$[33] and 3-formylsalicylic acid[34] were prepared following the methods reported in the literature.

Methods: Elemental analyses of the ligands and complexes were obtained using an Elementar model Vario-EI-III instrument. IR spectra were recorded as KBr pellets on a Nicolet NEXUS Aligent 1100 FT-IR spectrometer. Electronic spectra of the polymer-anchored compounds were recorded in Nujol on a Shimadzu1601 UV/Vis spectrophotometer by layering a mull of the sample inside one of the cuvettes while keeping other one layered with Nujol as a reference. The spectra of other ligands and complexes were recorded in methanol or DMF. ^{1}H NMR spectra were obtained using a Bruker 500 NMR spectrometer in $[D_6]$DMSO. EPR spectra were

recorded at room temperature on a Bruker EMX X-band spectrometer operating at 100-kHz field modulation at room temperature. The microwave frequency was calibrated using a frequency counter of the Microwave Bridge ER 041 XG-D. The Bruker Simfonia software package was used in the spectroscopic simulations and to calculate hyperfine coupling constant. The magnetic susceptibilities of simple oxidovanadium(IV) complexes were measured at 298 K with a Vibrating Sample Magnetometer model 155, using nickel as a standard. Diamagnetic corrections were carried out using Pascal's increments.[35] Thermogravimetric analyses of the complexes were carried out using a Perkin–Elmer (Pyris Diamond) instrument. Scanning Electron Micrographs (SEM) of polymer anchored ligands and complexes were recorded on a Leo instrument model 435 VP. The samples were coated with a thin film of gold to prevent the surface changing and to protect the surface material from thermal damage by the electron beam.

Preparations

H_2fsal-ea (I): A stirred solution of 2-aminoethanol (0.61 g, 10 mmol) in acetonitrile (10 mL) was added to a solution of 3-formylsalicylic acid (1.66 g, 10 mmol) in hot acetonitrile (30 mL) and the reaction mixture was heated to reflux on a water bath for 5 h. After reducing the solvent volume to ca. 10 mL, the flask was kept at room temperature. A yellow solid of **I** slowly separated out overnight. This was filtered, washed with petroleum ether and dried in vacuo. Yield 72%. $C_{10}H_{11}NO_4$ (209.2): calcd. C 57.40, H 5.30, N 5.70; found C 57.43, H 5.32, N 5.68. IR (KBr): $\tilde{\nu}_{max}$ = 1658 ($\nu_{C=O}$) cm^{-1}. ^1H NMR ([D$_6$]DMSO): δ = 12.89 (br., 1 H, carboxylic –OH), 5.20 (br., 1 H, phenolic OH), 8.37 (s, 1 H, –CH=N–), 8.09 (d, 1 H, aromatic), 7.69 (d, 1 H, aromatic), 6.75 (t, 1 H, aromatic), 3.77 (s, 2 H, –CH_2–), 3.70 (s, 2 H, –CH_2–) ppm. ^{13}C NMR ([D$_6$]DMSO): δ = 190.1 (carboxyl), 175.2 (azomethine), 168.4 (phenolic), 141.1, 139.9, 119.5, 116.1, 114.2 (aromatic), 59.3, 54.2 (alkyl chain) ppm.

H_2fsal-pa (II) and H_2fsal-amp (III): These ligands were prepared following the above procedure using 3-formylsalicylic acid (1.66 g, 10 mmol) and 3-aminopropanol (0.89 g, 10 mmol) or 2-amino-2-methylpropanol (0.89 g, 10 mmol).

Data for II: Yield 55%. $C_{11}H_{13}NO_4$ (223.2): calcd. C 59.17, H 5.87, N 6.28; found C 59.39, H 5.84, N 6.23. IR (KBr): $\tilde{\nu}_{max}$ = 1657 ($\nu_{C=O}$) cm^{-1}. ^1H NMR ([D$_6$]DMSO): δ = 12.09 (br., 1 H, carboxylic –OH), 4.80 (br., 1 H, phenolic –OH), 8.76 (s, 1 H, –CH = N–), 8.08 (d, 1 H, aromatic), 7.65 (d, 1 H, aromatic), 6.67 (t, 1 H, aromatic), 3.81 (t, 2 H, –CH_2–), 3.53 (t, 2 H, –CH_2–), 1.89 (quin, 2 H, –CH_2) ppm. ^{13}C NMR ([D$_6$]DMSO): δ = 190.8 (carboxyl), 175.2 (azomethine), 168.4 (phenolic), 141.0, 139.8, 119.5, 116.1, 114.1 (aromatic), 58.4, 49.7, 32.1 (alkyl chain) ppm.

Data for III: Yield 60%. $C_{12}H_{15}NO_4$ (237.2): calcd. C 60.73, H 6.38, N 5.91; found C 60.60, H 6.31, N 5.94. IR (KBr): $\tilde{\nu}_{max}$ = 1680 ($\nu_{C=O}$) cm^{-1}. ^1H NMR ([D$_6$]DMSO): δ = 13.57 (br., 1 H, carboxylic –OH), 5.57 (br., 1 H, phenolic –OH), 8.81 (s, 1 H, –CH = N–), 8.84 (d, 1 H, aromatic), 7.79 (d, 1 H, aromatic), 6.71 (t, 1 H, aromatic), 3.49 (s, 2 H, –CH_2–), 1.42 (s, 3 H, –CH_3), 1.17 (s, 3 H, –CH_3) ppm. ^{13}C NMR ([D$_6$]DMSO): δ = 190.1 (carboxyl), 168.2 (azomethine), 165.7 (phenolic), 141.2, 139.7, 119.4, 116.2, 114.2 (aromatic), 68.0, 61.2 (alkyl chain), 23.2 (methyl) ppm.

PS-H_2fsal-ea (IV): The polymer-anchored ligand PS-H_2fsal-ea was prepared following the procedure developed by Syamal et al.[36] Chloromethylated polystyrene (3.0 g) was allowed to swell in DMF (30 mL) for 2 h. A solution of H_2fsal-ea (9.96 g, 45 mmol) in DMF (30 mL) was added to the above suspension followed by triethylamine (4.50 g, 45 mmol) in ethyl acetate (50 mL). The reaction mixture was heated in an oil bath at 80 °C for 20 h with mechanical stirring. After cooling to room temperature, the yellow resins were filtered, washed thoroughly with hot DMF followed by hot methanol and dried in an air oven at 120 °C. Found: C 70.76, H 8.64, N 3.16. IR (KBr): $\tilde{\nu}_{max}$ = 1675 ($\nu_{C=O}$), 1635 ($\nu_{C=N}$) cm^{-1}.

PS-H_2fsal-pa (V) and PS-H_2fsal-amp (VI): The ligands PS-H_2fsal-pa and PS-H_2fsal-amp were prepared by following the procedure out lined for PS-H_2fsal-ea.

Data for V: Found: C 71.58, H 8.63, N 3.25. IR (KBr): $\tilde{\nu}_{max}$ = 1675 ($\nu_{C=O}$), 1637 ($\nu_{C=N}$) cm^{-1}.

Data for VI: Found: C 69.21, H 7.43, N 3.05. IR (KBr): $\tilde{\nu}_{max}$ = 1673 ($\nu_{C=O}$), 1630 ($\nu_{C=N}$) cm^{-1}.

[VO(fsal-ea)]$_2$ (1): A stirred solution of H_2fsal-ea (1.05 g, 5 mmol) in acetonitrile (30 mL) was added with stirring to [VO(acac)$_2$] (1.33 g, 5 mmol) dissolved in acetonitrile (25 mL) and the resultant reaction mixture was heated to reflux on a water bath for 3 h. After cooling to room temperature, a green precipitate of **1** was filtered, washed with acetonitrile and dried in vacuo. Yield 78%. $C_{10}H_9NO_5V$ (274.13): calcd. C 43.80, H 3.31, N 5.11, V 18.59; found C 43.62, H 3.42, N 5.05, V 18.06. IR (KBr): $\tilde{\nu}_{max}$ = 1670 ($\nu_{C=O}$), 1607 ($\nu_{C=N}$), 987 ($\nu_{V=O}$) cm^{-1}.

[VO(fsal-pa)]$_2$ (2) and [VO(fsal-amp)]$_2$ (3): Complexes **2** and **3** were prepared analogously to **1**, replacing H_2fsal-ea for H_2fsal-pa and H_2fsal-amp, respectively.

Data for 2: Yield 76%. $C_{11}H_{11}NO_5V$ (288.15): calcd. C 45.83, H 3.85, N 4.86, V 17.69; found C 45.91, H 3.65, N 4.74, V 17.14. IR (KBr): $\tilde{\nu}_{max}$ = 1673 ($\nu_{C=O}$), 1603 ($\nu_{C=N}$), 985 ($\nu_{V=O}$) cm^{-1}.

Data for 3: Yield 70%. $C_{12}H_{13}NO_5V$ (302.18): calcd. C 47.68, H 4.34, N 4.64, V 16.87; found C 47.30, H 4.54, N 4.41, V 16.36. IR (KBr): $\tilde{\nu}_{max}$ = 1674 ($\nu_{C=O}$), 1600 ($\nu_{C=N}$), 988 ($\nu_{V=O}$) cm^{-1}.

PS-[VO(fsal-ea)·DMF] (4): Polymer-anchored ligand PS-H_2fsal-ea (2.0 g) was allowed to swell in DMF (30 mL) for 2 h. A solution of [VO(acac)$_2$] (5.30 g, 20 mmol) in DMF (20 mL) was added to the above suspension and the reaction mixture was heated at 90 °C in an oil bath for 15 h while slow mechanical stirring. The blackish green beads of polymer-anchored complex **4** were filtered off, washed with hot DMF followed by hot methanol and dried at 120 °C in an air oven. Found: C 67.08, H 7.74, N 5.04, V 8.5. IR (KBr): $\tilde{\nu}_{max}$ = 1655 ($\nu_{C=O}$), 1607 ($\nu_{C=N}$), 977 ($\nu_{V=O}$) cm^{-1}.

PS-[VO(fsal-pa)·DMF] (5) and PS-[VO(fsal-amp)·DMF] (6): Complexes **5** and **6** were prepared by following the procedure out lined for **4**.

Data for 5: Found: C 68.18, H 7.86, N 4.83, V 7.93. IR (KBr): $\tilde{\nu}_{max}$ = 1659 ($\nu_{C=O}$), 1609 ($\nu_{C=N}$), 993 ($\nu_{V=O}$) cm^{-1}.

Data for 6: Found: C 64.19, H 7.31, N 4.66, V 7.26. IR (KBr): $\tilde{\nu}_{max}$ = 1675 ($\nu_{C=O}$), 1609 ($\nu_{C=N}$), 964 ($\nu_{V=O}$) cm^{-1}.

Catalytic Activity Studies

Oxidation of Styrene: The oxidation of styrene was carried out in a 50 mL reaction flask fitted with a water condenser. All anchored catalysts were allowed to swell in acetonitrile for 2 h prior to their use. In a typical oxidation reaction, styrene (1.04 g, 10 mmol) and aqueous 30% H_2O_2 (2.27 g, 20 mmol) were mixed in acetonitrile (10 mL) and the reaction mixture was heated to 80 °C with stirring. The appropriate catalyst (0.040 g) was added to the reaction mixture and stirred for 6 h. The progress of the reaction was monitored by withdrawing small amounts of the reaction mixture at different time intervals and analysing them quantitatively by gas chromatography. The identities of the products were confirmed by GC–MS

(Perkin–Elmer, Clarus 500). The effects of various parameters such as temperature, amount of oxidant and catalyst were studied to obtain suitable reaction conditions for the best performance of the catalyst.

Oxidation of Cumene: Cumene (1.20 g, 10 mmol), 30% aqueous H_2O_2 (2.26 g, 20 mmol) and anchored catalyst (0.060 g), after swelling in acetonitrile as stated above in acetonitrile (10 mL), were heated at 80 °C with stirring and the reaction was monitored as mentioned above. Various parameters such as amount of oxidant and catalyst and temperature of the reaction were considered to see their effect on the reaction products. However, the basic procedure was the same as outlined above.

Supporting Information (see also the footnote on the first page of this article): Electronic spectral data (Table S1) and electronic spectra of neat and polymer-anchored oxidovanadium(IV) complexes (Figue S1).

Acknowledgments

U. K. is thankful to the University Grant Commission (New Delhi, India) for Senior Research Fellowship and M. R. M. thanks the Council of Scientific and Industrial research (New Delhi, India) for financial support of the work. The authors are also thankful to Thermax Limited Pune, India, for generous gift of chloromethylated polystyrene.

[1] a) A. Messerschmidt, R. Wever, *Proc. Natl. Acad. Sci. USA* **1996**, *93*, 392–396; b) S. Macedo-Ribeiro, W. Hemrika, R. Renirie, R. Wever, A. Messerschmidt, *J. Biol. Inorg. Chem.* **1999**, *4*, 209–219.
[2] a) I. Harvey, J. M. Arber, R. R. Eady, B. E. Smith, C. D. Garner, S. S. Hasnain, *Biochem. J.* **1990**, *266*, 929–931.
[3] a) A. N. Antipov, D. Y. Sorokin, N. P. L'Lov, J. G. Kuenen, *Biochem. J.* **2003**, *369*, 185–189; b) A. N. Antipov, N. M. Lyalikova, T. V. Khilniak, N. P. L'Lov, *FEBS Lett.* **1998**, *441*, 257–260.
[4] a) G. J. Colpas, B. J. Hamstra, J. W. Kampf, V. L. Pecoraro, *J. Am. Chem. Soc.* **1996**, *118*, 3469–3478; b) B. J. Hamstra, G. J. Colpas, V. L. Pecoraro, *Inorg. Chem.* **1998**, *37*, 949–955.
[5] a) A. Butler, *Coord. Chem. Rev.* **1999**, *187*, 17–35; b) D. Rehder, *Coord. Chem. Rev.* **1999**, *182*, 297–322.
[6] M. R. Maurya, *Coord. Chem. Rev.* **2003**, *237*, 163–181.
[7] a) V. Conte, F. DiFuria, G. Licini, *Appl. Catal. A* **1997**, *157*, 335–361; b) A. G. J. Ligtenbarg, R. Hage, B. L. Feringa, *Coord. Chem. Rev.* **2003**, *237*, 89–101; c) C. Bolm, *Coord. Chem. Rev.* **2003**, *237*, 245–256.
[8] a) T. S. Smith II, V. L. Pecoraro, *Inorg. Chem.* **2002**, *41*, 6754–6760; b) A. Butler, M. J. Clague, G. E. Meister, *Chem. Rev.* **1994**, *94*, 625–638; c) H. B. ten Brink, A. Tuynman, H. L. Dekker, W. Hemrika, Y. Izumi, T. Oshiro, H. E. Schoemaker, R. Wever, *Inorg. Chem.* **1998**, *37*, 6780–6784; d) M. Andersson, A. Willetts, S. Allenmark, *J. Org. Chem.* **1997**, *62*, 8455–8458; e) V. M. Dembitsky, *Tetrahedron* **2003**, *59*, 4701–4720; f) D. Rehder, G. Santoni, G. M. Licini, C. Schulzke, B. Meier, *Coord. Chem. Rev.* **2003**, *237*, 53–63.
[9] M. R. Maurya, U. Kumar, P. Manikandan, *Dalton Trans.* **2006**, 3561–3575.
[10] a) B. Meunier, *Chem. Rev.* **1992**, *92*, 1411–1456; b) D. C. Sherrington, in *Supported Reagents and Catalyst in Chemistry* (Ed.: B. K. Hodnett, A. P. Keybett, J. H. Clark, K. Smith), Royal Society of Chemistry, Cambridge, **1998**, p. 220.
[11] R. Ando, T. Yagyu, M. Maeda, *Inorg. Chim. Acta* **2004**, *357*, 2237–2244.
[12] A. Syamal, K. S. Kale, *Inorg. Chem.* **1979**, *18*, 992–995.
[13] A. Syamal, K. S. Kale, *Indian J. Chem., Sect. A* **1980**, *19*, 225–228.
[14] A. Syamal, E. F. Carey, L. J. Theriot, *Inorg. Chem.* **1973**, *12*, 245–248.
[15] C. J. Carrano, C. M. Nunn, R. Quan, J. A. Bonadies, V. L. Pecoraro, *Inorg. Chem.* **1990**, *29*, 944–951.
[16] P. Arroyo, S. Gil, A. Munoz, P. Palanca, J. Sanchos, V. Sanz, *J. Mol. Catal. A* **2000**, *160*, 403–408.
[17] P. S. Gahlot, A. Agarwal, V. P. Seth, S. Sanghi, S. K. Gupta, M. Arora, *Spectrochim. Acta, Part A* **2005**, *61*, 1189–1194.
[18] A. Bruckner, H. W. Zanthoff, *Colloids Surf., A* **1999**, *158*, 107–113.
[19] V. Hulea, E. Dumitriu, *Appl. Catal. A* **2004**, *277*, 99–106.
[20] M. R. Maurya, M. Kumar, S. Sikarwar, *React. Funct. Polym.* **2006**, *66*, 808–818.
[21] Z. Fu, D. Yin, Q. Li, L. Zhang, Y. Zhang, *Microporous Mesoporous Mater.* **1999**, *29*, 351–359.
[22] M. R. Maurya, S. Sikarwar, T. Joseph, P. Manikandan, S. B. Halligudi, *React. Funct. Polym.* **2005**, *63*, 71–83.
[23] S. Matsui, T. Fujita, *Catal. Today* **2001**, *71*, 145–152.
[24] S. L. H. Rebelo, M. M. Q. Simoes, M. G. P. M. S. Neves, J. A. S. Cavalerio, *J. Mol. Catal. A* **2003**, *201*, 9–22.
[25] E. N. Panayotova-Björnbom, D. I. Dimitrov, M. P. Popangelova, A. A. Petkov, *J. Catal.* **1980**, *62*, 79–83.
[26] G. R. Verma, W. F. Graydon, *J. Catal.* **1973**, *28*, 236–244.
[27] a) A. K. Agarwal, R. D. Sristava, *J. Catal.* **1976**, *45*, 86–93; b) L. V. G. Krishna, M. S. Rao, R. D. Srivastava, *J. Catal.* **1977**, *49*, 109–111.
[28] a) S. Vetrivel, A. Pandurangan, *J. Mol. Catal. A* **2005**, *227*, 269–278; b) S. Vetrivel, A. Pandurangan, *Catal. Lett.* **2004**, *95*, 167–177.
[29] Y. F. Hsu, C. P. Cheng, *J. Mol. Catal. A* **1998**, *136*, 1–11.
[30] a) Y.-F. He, R.-M. Wang, Y.-Y. Liu, Y. Chang, Y.-P. Wang, C.-G. Xia, J.-S. Suo, *J. Mol. Catal. A* **2000**, *159*, 109–113; b) R.-M. Wang, S.-B. Li, Y.-P. Wang, Y. Chang, Y.-F. He, Z.-Q. Lei, H.-X. Feng, *React. Funct. Polym.* **1999**, *42*, 87–92.
[31] E. Baciocchi, F. d'Acunzo, C. Galli, M. Loele, *J. Chem. Soc., Chem. Commun.* **1995**, 429–430.
[32] M. R. Maurya, S. Khurana, E. Schulzke, D. Rehder, *Eur. J. Inorg. Chem.* **2001**, 779–788.
[33] R. A. Row, M. M. Jones, *Inorg. Synth.* **1957**, *5*, 113 –116.
[34] J. C. Duff, E. J. Bills, *J. Chem. Soc.* **1923**, 1987.
[35] R. L. Dutta, A. Syamal, *Elements of Magnetochemistry*, 2nd ed., Affiliated East-West Press, New Delhi, **1993**, p. 8.
[36] A. Syamal, M. M. Singh, *Indian J. Chem., Sect. A* **1992**, *31*, 110–115.

Received: November 29, 2006
Published Online: April 24, 2007

